

# Development of a Double-Sided Consequent Pole Linear Vernier Hybrid Permanent-Magnet Machine for Wave Energy Converters

A. A. Almoraya, N. J. Baker, K. J. Smith and M. A. H. Raihan

Electrical Power Research Group, School of Electrical and Electronic Engineering, Newcastle University  
Newcastle upon Tyne, NE17RU, UK  
a.a.a.almoraya@ncl.ac.uk

**Abstract**—Wave energy conversion can be simplified by using direct drive linear generators which may improve reliability. Numerous topologies of direct drive linear generators have been proposed in the last few decades such as the linear vernier hybrid permanent magnet (LVHPM) machine. However, the cost of this kind of machine is driven by the quantity of permanent magnet (PM) material. This paper proposes a linear vernier hybrid permanent magnet machine with consequent pole and concentrated windings for wave energy converters, which requires less magnet material for comparable performance. The key of the proposed design is the modular stator where the unbalanced magnetic circuit caused by consequent pole can be eliminated. Based on finite element analyses (FEA) the present machine is capable of higher thrust force, higher back EMF and lower cogging force as well as force ripple compared to that of a baseline LVHPM machine.

**Keywords**—consequent pole; linear vernier hybrid PM ; wave energy.

## I. INTRODUCTION

In recent years, low speed linear permanent magnet machines have been widely used in direct-drive applications such as wave energy conversion and rope-less lifts, in which the mechanical interface can be excluded[1].

Direct-Drive-Wave Energy Converters (DD-WECs) are systems where the moving part of the converter, such as the buoy or wave swing, is coupled directly to the moving part of the linear generator, the translator. The stator is installed on the seabed or other inertial reference and the wave energy conversion can be performed by the relative motion between translator and stator. Proposed wave energy devices using a direct drive linear generator include the Archimedes wave swing [2] and heaving buoy [3]. Due to the absence of the mechanical intermediate between low speed prime mover and high speed generator, the DD-WEC has the merit of high efficiency, low capital and maintenance costs. However, due to the low speed operation of the linear generator in DD-WEC, its huge size and large number of poles are considered as a critical issue[4].

In [5, 6], a linear magnetic-gear permanent magnet (PM) machine for DD-WEC was proposed, where a linear magnetic gear was artificially combined with a linear PM machine. Consequently, both low speed and high speed machine design can be attained. However, it suffers from complexity of manufacturing since it includes three airgaps, two movers and an extra length produced by the integration between magnetic gear and PM machine. A transverse flux permanent magnet machine is regarded as one of the most the favorable machines for direct drive system due to its high shear stress density [7], this class of machine was also advanced for DD-WEC [8]. However, the three-dimensional flux route make it complicated to be designed and built [9]. A vernier PM machine was developed for direct drive applications[10]. The equivalent linear type was also proposed for DD-WEC[11]. In [12] a linear vernier hybrid machine was proposed for DD-WEC which is capable to produce shear stress up to 250kN/m<sup>2</sup>. However, an alternating polarity arrangement of PMs is used in this machine which result in half of PMs generating the main flux while the leakage flux is produced by the remaining PMs. Therefore, a significant proportion of the machine cost results from the inefficient use of PM material. A linear vernier PM machine with consequent pole, distributed windings and non-modular stator was proposed where 30% of the PM material can be saved [13]. However, since large end windings is needed the copper losses may be increased.

This paper presents a double-sided LVHPM machine with a modular stator and concentrated windings. The consequent pole technique is adopted in the new design which halves the amount of the PM material leading to a significant reduction in the initial cost of the generator. The performance of the machine would not be sacrificed by implementing this topology [14]. This class of machine can offer higher average force, higher no-load back EMF, while it exhibits lower cogging force and force ripple compared to that of the baseline LVHPM machine. In addition, with the use of tapered ferromagnetic poles (FP) sinusoidal back EMF waveforms can be obtained.

The proposed model also offers special advantages over the baseline LVHPM machine:

---

The authors acknowledge financial support from Technical and Vocational Training Corporation, Saudi Arabia.

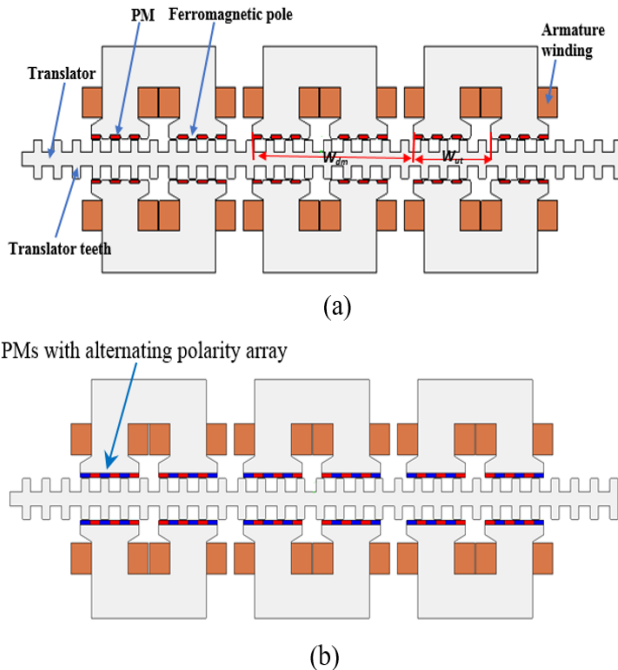


Fig. 1 Structure of LVHPM machine (a) proposed, (b) baseline

- Since modular primary configuration separates each phase magnetically, the stator can be physically segmented for specific applications.
- Due to the adoption of the modular stator assembly the unbalanced magnetic circuit can be suppressed [15]
- Consequent pole minimizes the fringing flux leading to an increase in the main flux[15].
- Tapered ferromagnetic poles can reduce the flux leakage and hence the effective flux increases consequently.

## II. DESCRIPTION OF THE PROPOSED LVHPM TOPOLOGY

Fig.1 (a) illustrates the configuration of the proposed three-phase double-sided LVHPM machine. Each side is composed of three U-shaped laminated cores with six stator teeth. The surface of these teeth accommodates three PMs with the same magnetization orientation. The key difference between the new design and the baseline LVHPM machine is that one polarity

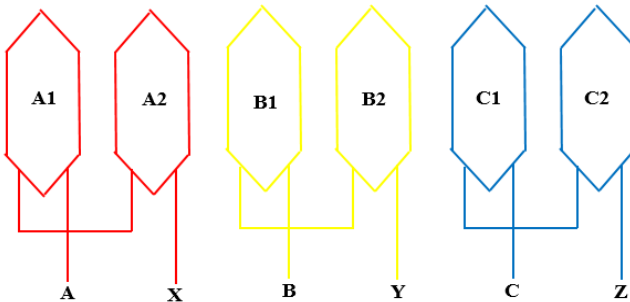


Fig. 2: Upper side winding arrangement

TABLE I: PARAMETERS OF THE BASELINE AND PROPOSED LVHPM MACHINES

Parameters	value	
	baseline	proposed
Number of phases	3	
Rated speed, m/s	1	
Air gap length, mm	1	
PM width, mm	12	
PM thickness, mm	4	
Stack length, mm	100	
Secondary pole pitch, $\tau_s$ , mm	24	
Number of turns	145	
PM number/ primary tooth	6	3
Rated current, A	14.2	
PM remanence	1.2 T	
PM material	NdFeB	
Stator and translator core	Laminated steel	

of PMs is missing and replaced with tapered FPs. In other words, the structure of the proposed model has the same polarity either north or south, while alternating adjacent polarity is adopted in the baseline design as shown in Fig.1 (b).The translator which is sandwiched between both stator sides is formed of an iron core with salient teeth on the two sides which strengthen the transmission of the thrust force.

Single tooth concentrated windings are employed in the proposed machine, in which four coils make one phase and adjacent coils in each C-core are reversely connected. Fig.2 shows the upper side armature winding arrangement.

Since the new design possess almost the same structure of the baseline LVHPM machine, the magnet width is equal to half of the translator tooth pitch. The relative displacement between the teeth of the U-shaped module is 360 electrical degrees, given by

$$W_{ut} = (m+F+2n) W_{pm} \quad (1)$$

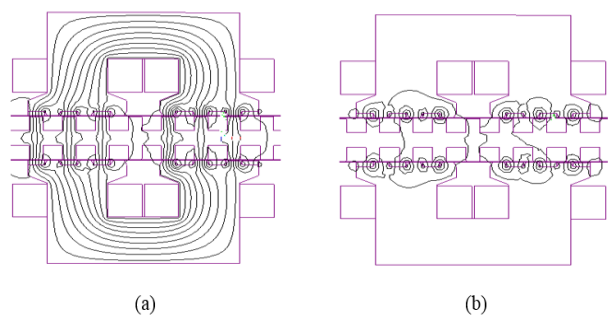


Fig. 3: No load magnetic field distributions  
(a) aligned position,  $\Theta = 0^\circ$ , (b) unaligned position,  $\Theta = 90^\circ$

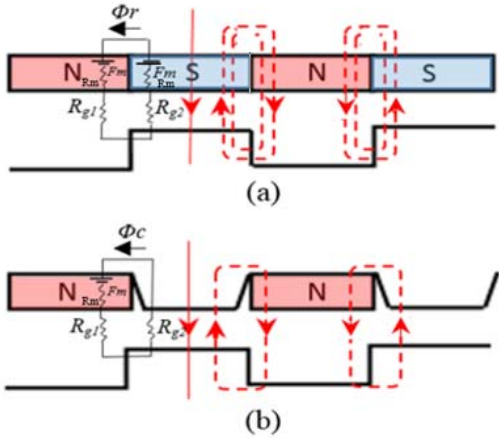


Fig. 4: Diagrams of reluctance path and flux lines of two structures  
(a) baseline LVHPM machine, (b) the proposed LVHPM machine

where,  $W_{ut}$  is the space between the teeth of the U-shaped module,  $W_{pm}$  is the width of the PM,  $m$  is the number of PMs,  $F$  is the number of ferromagnetic poles and  $n$  is an integer. In addition, the mechanical displacement  $W_{dm}$  between the adjacent U-shaped modules should match 120 electrical degrees to obtain a three phase machine, and that can be achieved by making this space satisfy,

$$W_{dm} = (n \pm 1/3)\tau \text{ or } (n \pm 1/6)\tau \quad (2)$$

where  $n$  is a positive integer.

The main parameters for the baseline [12] and proposed LVHPM machines are listed in table I.

### III. PRINCIPLE OF OPERATION

The proposed machine has the same operation principle as the baseline LVHPM machine. When the translator teeth are aligned with PMs and ferromagnetic poles, the flux linkage across the coils achieves its peak value as illustrated in Fig.3 (a). The flux linkage decreases with displacement, reaching zero at the unaligned position, as illustrated in Fig.3 (b). Flux is reversed when the mover reaches the next alignment position. Hence, the flux linkage polarity is rapidly changed over a small translator movement which may contribute to improve the

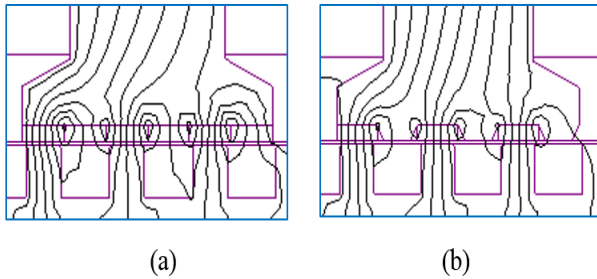


Fig. 5: flux line plot (a) baseline LVHPM machine (b) proposed LVHPM machine

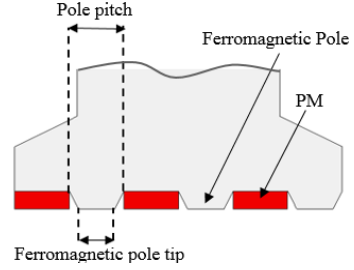


Fig.6 Module of stator

thrust force density. This phenomenon is known as “magnetic gearing effect” [5].

Fig.4 shows the slot and PM configurations of the baseline and proposed LVHPM machines. It can be noticed that the width of PM pole pitch and slot are equal, and so the main flux is produced by only half of the PMs, whilst the remaining PMs cause the leakage. As it can be seen in the aforementioned figure that, the main flux is generated by the south pole PMs, and the leakage flux is made by the north pole PMs. It can be also deducted that some flux excited by the S-pole PMs travel through the air gap toward the primary teeth and then pass through the tooth edges to the N-pole PMs instead of linking the stator coil. The flux leakage for the baseline LVHPM machine and the consequent pole version can be defined as:

$$\Phi_r = \frac{Fm}{\frac{Rg1 + Rg2}{2} + Rm} \quad (3)$$

$$\Phi_c = \frac{Fm}{Rg1 + Rg2 + Rm} \quad (4)$$

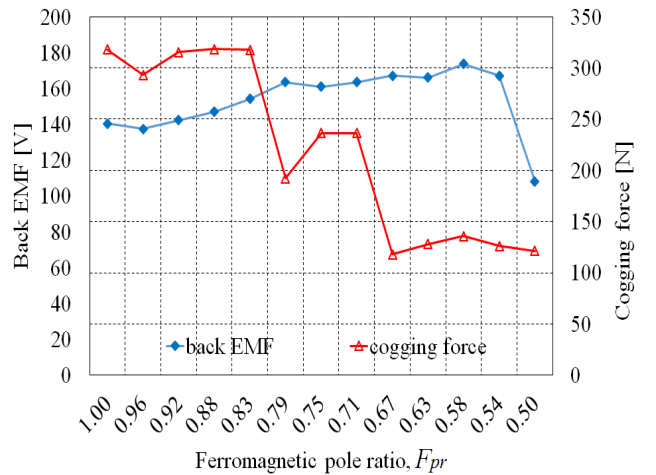


Fig. 7: variation of the no-load back EMF and cogging force with respect to the ferromagnetic pole ratio ( $F_{pr}$ )

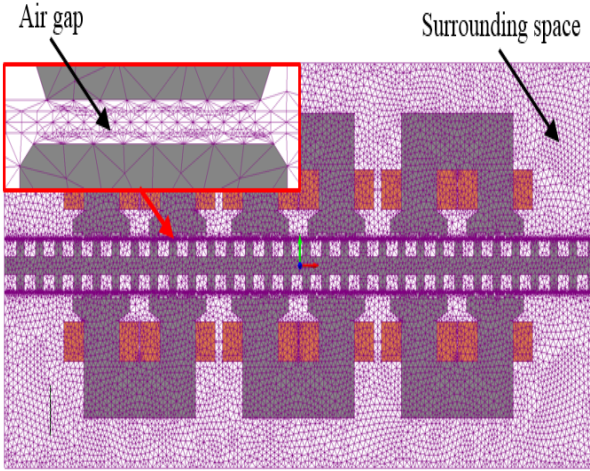


Fig. 8: Generated mesh for the proposed LVHMPM model

where  $R_{g1}$  and  $R_{g2}$  are the slot air gap reluctance and tooth air gap reluctance respectively,  $R_m$  is the PM reluctance,  $\Phi_r$  is the flux leakage for the baseline LVHMPM machine and  $\Phi_c$  is the flux leakage for the proposed LVHMPM machine. From (3) and (4) it is clear that the flux leakage of the proposed design  $\Phi_c$  which adopts the consequent pole is smaller than that of the conventional LVHMPM machine  $\Phi_r$  ( $\Phi_c < \Phi_r$ ). Thus, the effective flux produced by the proposed design is higher than that of the baseline one where only 50% of PM material is used. The tapered FPs can reduce the leakage flux further compared to that of rectangular FPs as illustrated in Fig. 5 (b). An equivalent analysis for a rotary version of vernier hybrid PM machine (VHPM) and (VHPM) with consequent pole was conducted in [16].

The flux lines plots produced by 2D-FEA for both baseline LVHMPM and the consequent pole version are illustrated in Fig.5. Both designs have the same structure, and dimensions except the missing PMs that were replaced with tapered FPs. It can be seen that the proposed LVHMPM design has a lower pole to pole leakage flux than that of the baseline one, validating the assumptions used in (3) and (4). Thus, the main flux of the latter design is greater than that of the baseline LVHMPM.

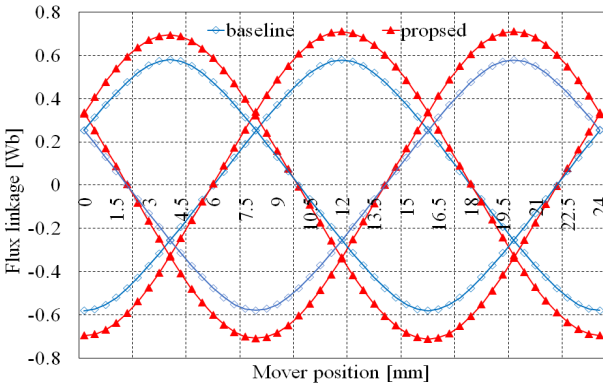


Fig. 9: no-load flux linkage waveforms of both machines

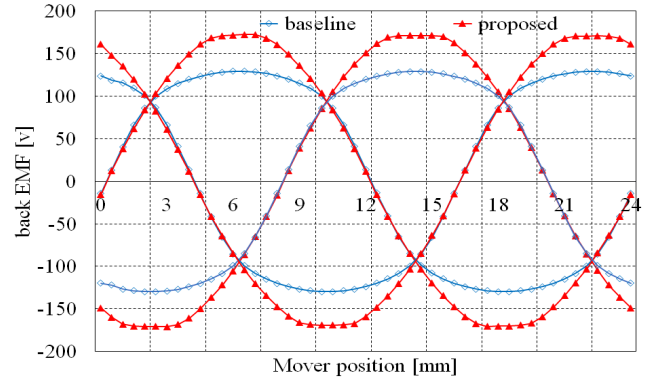


Fig. 10: no-load back EMF waveforms of both machines

#### IV. DESIGN OPTIMIZATION

Tapered ferromagnetic poles are adopted in the new design which have a noticeable impact on the fringing flux reduction as clarified in the next section. Therefore, the ferromagnetic pole ratio  $F_{pr}$  can affect the performance of the proposed LVHMPM machine such as cogging force and no-load back EMF and its waveform shape. Thus, the optimization of the ratio between ferromagnetic pole tip width  $f_t$  to the pole pitch  $\tau$  which is shown in Fig.6 is an important stage of the machine design.

Fig.7 shows the effect of varying ferromagnetic pole ratio on the no-load back EMF and cogging torque. It can be seen that the peak no-load back EMF can be achieved when  $F_{pr}$  equals to 0.58 with the value of 173.6 V. However, the ratio of 0.67 was selected where the lowest value of the cogging force can be attained and the peak no-load EMF remaining at an acceptable high value of 167 V.

#### V. SIMULATION RESULTS

In order to analyze the operation principle of the proposed LVHMPM machine the no-load flux density has been calculated by means of FEA, 1.22 T. The end effect has been considered in which the model has been surrounded by appropriate air space as shown in Fig.8. In addition, four mesh layers are created in the air gap in order to obtain accurate calculated results.

##### A. flux linkage and no-load back EMF

In order to evaluate the validity of the comparison between the proposed LVHMPM machine and the baseline LVHMPM machine, they were designed based on the same key dimensions: number of phases, rated speed, number of turns per phase and translator pole pitch. Fig. 9 compares the no-load flux linkage waveforms for both machines. It can be seen that the proposed LVHMPM machine offers higher flux linkage than that of the baseline LVHMPM machine. In addition, the induced no-load back EMF is also greater under the same speed condition as shown in Fig.10. The generated open-circuit back EMF at rated speed is 129 V and 167 V for the baseline and proposed LVHMPM machine respectively. Hence, a 23% higher

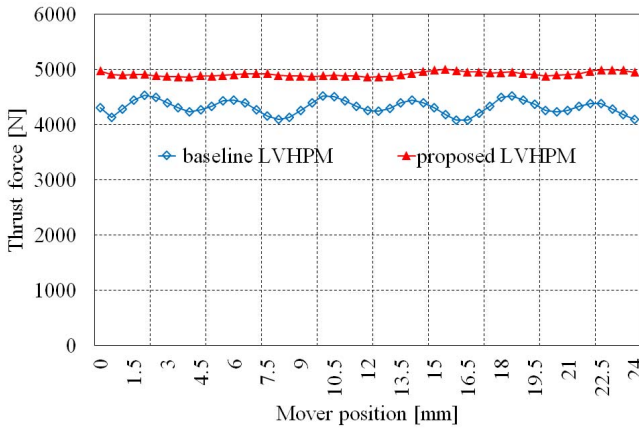


Fig.11: Thrust force waveforms of both machines

no-load back EMF is produced using only 50% of the PM material. As can be seen in Fig.9 the flux linkage waveforms for the proposed LVHPM machine are symmetrical, balanced and sinusoidal resulting in sinusoidal no-load back EMF which may improve the converter performance and hence the system efficiency. The induced back EMF can be defined as:

$$e = \frac{d\psi m}{dt} = \frac{d\psi m}{dx} \cdot \frac{dx}{dt} = \frac{d\psi m}{dx} \cdot v \quad (5)$$

### B. Thrust force

Fig.11 shows the thrust force waveforms for the baseline and proposed LVHPM machines under the rated armature current of 14.2 A<sub>–</sub> (RMS). The applied current is assumed to be sinusoidal which smoothes the obtained thrust force waveforms. In this paper, the ratio of the peak to peak force to the average force is defined as force ripple which can be given by:

$$\text{Force ripple} = \frac{F_{\max} - F_{\min}}{F_{\text{avg}}} \times 100 \quad (6)$$

where  $F_{\max}$ ,  $F_{\min}$  and  $F_{\text{avg}}$  are the maximum value, minimum value and average value of the thrust force respectively.

TABLE II: THRUST CONSTANT AND RIPPLE OF BOTH MODELS

Phase current [A]	Current density [A/mm <sup>2</sup> ]	Thrust constant/[N/A]/ripple [%]			
		Baseline LVHPM		Proposed LVHPM	
2.83	0.92	305	46.3	383.2	12
5.67	1.84	305.4	23.3	375	5.5
8.51	2.76	305.6	16	375.8	3.8
11.34	3.69	305.9	12.7	364.3	2.9
14.2	4.6	305	10.6	348.5	2.86
17	5.5	304.9	9.1	322.4	4.6
19.8	6.4	303.7	7.8	297.4	7.6
Average		305	18	352.4	5.6

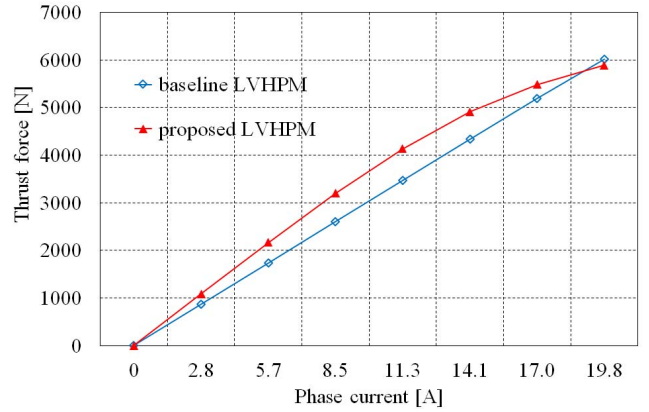


Fig. 12: Average force vs. phase current for both LVHPM machines

From the above-mentioned figure it can be seen that by adopting the consequent pole topology 12% extra thrust force can be obtained from the proposed LVHPM machine with a low level of force ripple, only 2.86 %, while an excessive force ripple of 10.6 % is produced by the baseline LVHPM machine when both machines are operated at the same speed and electric loading. Fig.12 illustrates the average force characteristics of the baseline and proposed LVHPM machines. It can be observed that in both machines as current increases, the average force increases almost linearly. However, in the proposed design saturation can be seen to start at a lower MMF as consequent pole structure gives a reduced magnetic air gap to the coil driven flux. For any fixed output force below 5000N, the consequent pole machine uses a lower current and will hence have lower I<sup>2</sup>R losses.

Table II summarizes the armature phase current, current density, ratio of the average force to the applied phase current which is defined as thrust constant and thrust ripple of the baseline and proposed LVHPM machines. Table III compares the baseline LVHPM machine with the proposed LVHPM in terms of no-load back EMF, thrust force and its ripple, cogging force. In addition, it also shows that the proposed design offers 12.5% higher thrust force density and 127.8% higher thrust force per magnet mass.

Based on the above analysis it can be observed that the proposed design needs only 50% of the magnet mass of that of its equivalent resulting in a lower initial cost. In fact the implementation of the iron poles in the proposed LVHPM machine reduces the effective airgap, and hence the equivalent magnetic reluctance is much less than that of the baseline

TABLE III: TRANSIENT FEA PERFORMANCE COMPARISON

Item	Unit	Baseline LVHPM	Proposed LVHPM
No-load back EMF	V	129	167
Cogging force pk-pk	N	397	118
Average thrust force	KN	4.3	4.95
Thrust force ripple	N	454	141
Thrust force density	KN/m <sup>3</sup>	335	383
Thrust force/PM mass	KN/kg	1.8	4.1

LVHPM machine. Consequently, the power density can be significantly improved by the proposed machine.

### C. Cogging force

Cogging force is an undesirable effect which may lead to mechanical vibration for PM linear generator. Therefore, minimizing cogging force is a vital requirement for PM machine design. Fig.13 depicts the cogging force waveforms for both the baseline and proposed LVHPM machines. It can be seen that the peak to peak cogging force of the proposed LVHPM machine is 118 N which is only 2.3% of the rated thrust force, while the peak to peak cogging force of the baseline LVHPM is 397 N. Which means, the proposed design exhibits much smaller cogging force than that of existing LVHPM machine, hence smoother thrust force is offered by the former machine, particularly at low speed operations. It should be also indicated that the proposed LVHPM machine produces low cogging force and force ripple without applying skewing technique which has been conducted in the existing studies [17, 18]. That is due to the implementation of the tapered ferromagnetic poles which have a great influence on the cogging force as discussed in section IV. Therefore, the new LVHPM machine possess the merit of simplicity of manufacturing.

## VI. CONCLUSION

A new class of modular LVHPM machine has been proposed in this paper which is suitable for direct-drive wave energy applications, in which the mass of PMs can be reduced by 50%. The present machine has been designed, analyzed and compared to the baseline LVHPM machine. The obtained results of the FEA indicate that the proposed LVHPM machine offers 23 % larger open-circuit back EMF and 12% higher thrust force while it exhibits lower cogging force and force ripple compared to the baseline LVHPM one under the same operation conditions. Therefore, by adopting the proposed topology the developed generator is more cost effective and force dense.

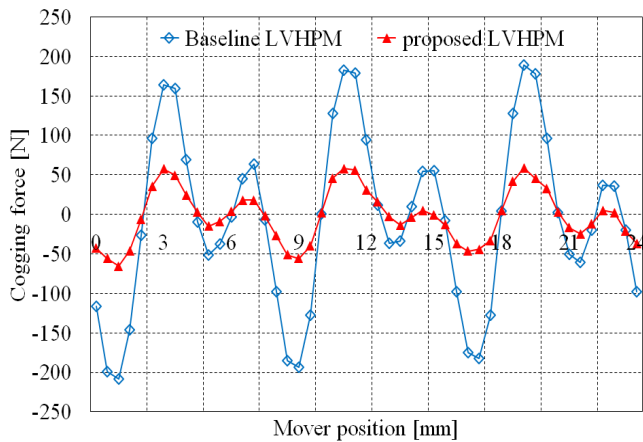


Fig. 13: Cogging force waveforms over a complete electrical cycle

## REFERENCES

- [1] N. Hodgins, O. Keysan, A. S. McDonald, and M. A. Mueller, "Design and testing of a linear generator for wave-energy applications," *IEEE Transactions on Industrial Electronics*, vol. 59, pp. 2094-2103, 2012.
- [2] H. Polinder, M. E. C. Damen, and F. Gardner, "Linear PM generator system for wave energy conversion in the AWS," *IEEE Transactions on Energy Conversion*, vol. 19, pp. 583-589, 2004.
- [3] M. Leijon, H. Bernhoff, O. Agren, J. Isberg, J. Sundberg, M. Berg, *et al.*, "Multiphysics simulation of wave energy to electric energy conversion by permanent magnet linear generator," *IEEE Transactions on Energy Conversion*, vol. 20, pp. 219-224, 2005.
- [4] P. R. M. Brooking and M. A. Mueller, "Power conditioning of the output from a linear vernier hybrid permanent magnet generator for use in direct drive wave energy converters," *IEE Proceedings-Generation, Transmission and Distribution*, vol. 152, pp. 673-681, 2005.
- [5] W. Li, K. T. Chau, and J. Z. Jiang, "Application of linear magnetic gears for pseudo-direct-drive oceanic wave energy harvesting," *IEEE Transactions on Magnetics*, vol. 47, pp. 2624-2627, 2011.
- [6] M. A. M. N.J. Baker, M.A.H. Raihan, "All electric drive train for wave energy power take off," presented at the IET Renewable power generation, 2016.
- [7] H. Weh, "Design of an integrated propulsion, guidance, and levitation system by magnetically excited transverse flux linear motor (TFM-LM)," *IEEE Transactions on Energy Conversion*, vol. 19, pp. 477-484, 2004.
- [8] H. Polinder, B. C. Mecrow, A. G. Jack, P. G. Dickinson, and M. A. Mueller, "Conventional and TFPMP linear generators for direct-drive wave energy conversion," *IEEE Transactions on Energy Conversion*, vol. 20, pp. 260-267, 2005.
- [9] A. M. El-Refaie, "Fault-tolerant permanent magnet machines: a review," *IET Electric Power Applications*, vol. 5, pp. 59-74, 2011.
- [10] A. Toba and T. A. Lipo, "Novel dual-excitation permanent magnet vernier machine," in *Industry Applications Conference, 1999. Thirty-Fourth IAS Annual Meeting. Conference Record of the 1999 IEEE*, 1999, pp. 2539-2544.
- [11] K.-T. Chau, W. Li, and C. H. T. Lee, "Challenges and opportunities of electric machines for renewable energy," *Progress In Electromagnetics Research B*, vol. 42, pp. 45-74, 2012.
- [12] M. A. Mueller and N. J. Baker, "Modelling the performance of the vernier hybrid machine," *IEE Proceedings-Electric Power Applications*, vol. 150, pp. 647-654, 2003.

- [13] X. Liu, C. Zou, Y. Du, and F. Xiao, "A linear consequent pole stator permanent magnet vernier machine," in *Electrical Machines and Systems (ICEMS), 2014 17th International Conference on*, 2014, pp. 1753-1756.
- [14] S.-U. Chung, Y.-D. Chun, B.-C. Woo, D.-K. Hong, and J.-Y. Lee, "Design considerations and validation of permanent magnet vernier machine with consequent pole rotor for low speed servo applications," *Journal of Electrical Engineering and Technology*, vol. 8, pp. 1146-1151, 2013.
- [15] S.-U. Chung, J.-W. Kim, B.-C. Woo, D.-K. Hong, J.-Y. Lee, and D.-H. Koo, "A novel design of modular three-phase permanent magnet vernier machine with consequent pole rotor," *IEEE transactions on magnetics*, vol. 47, pp. 4215-4218, 2011.
- [16] D. Li, R. Qu, J. Li, and W. Xu, "Design of consequent pole, toroidal winding, outer rotor vernier permanent magnet machines," in *2014 IEEE Energy Conversion Congress and Exposition (ECCE)*, 2014, pp. 2342-2349.
- [17] S.-U. Chung, H.-J. Lee, and S.-M. Hwang, "A novel design of linear synchronous motor using FRM topology," *IEEE Transactions on Magnetics*, vol. 44, pp. 1514-1517, 2008.
- [18] S.-U. Chung, H.-J. Lee, B.-C. Woo, J.-W. Kim, J.-Y. Lee, S.-R. Moon, et al., "A feasibility study on a new doubly salient permanent magnet linear synchronous machine," *IEEE Transactions on Magnetics*, vol. 46, pp. 1572-1575, 2010.